

RED HORIZONTAL BRANCH AND EARLY ASYMPTOTIC BRANCH STARS NEAR THE SUN

OLIN J. EGGEN

Cerro Tololo Inter-American Observatory, National Optical Astronomy Observatories,¹ Casilla 603, La Serena, Chile

Electronic mail: oeggen@noao.edu

Received 1997 May 12; revised 1997 June 25

ABSTRACT

Sixty one red horizontal branch (RHB) and early asymptotic branch (EAGB) stars are isolated. Heavy element abundances, from Strömgren photometry, and calcium abundances, from hk photometry, have been derived. The $(b-y)$ colors of these objects are apparently not appreciably affected by differential line-blanketing although abundance determination from the m_1 index of Strömgren photometry is apparently valid. The Ca abundance is derived from $P[Ca/h] = [hk(\text{obs}) - hk(\text{comp})]/0.362 + 0.10$ dex, where $hk(\text{comp}) = 1.55(b-y) + 0.335$. The overabundance of the α process element calcium, with respect to the heavy elements, that was noted elsewhere for halo giants and dwarfs, is also a feature of RHB and EAGB stars. The data from the best observed halo globular clusters lead to $M_v = 5.05 - 4.70(B-V) + [1.34 - 0.50(B-V)] [Fe/H]$ for the RHB and EAGB stars or $dM_v(\text{AGB})/d[Fe/H] = 0.84$ at $B-V = +1.0$ mag compared with 0.40 for the cluster variables in the same clusters. More recent determinations of moduli for several of the globular clusters (Reid 1997, ApJ, preprint) give values that are systematically 0.50–0.55 mag larger, effecting the zero point of the luminosity–color–abundance relation. Evidence for kinematic and abundance boundaries between disk and halo populations is discussed. © 1997 American Astronomical Society. [S0004-6256(97)00810-8]

Red horizontal branch (RHB) and asymptotic giant branch (AGB) stars have attracted much theoretical attention but observational studies of globular cluster RHB and AGB members are relatively scarce. The AGB consists of two parts, of which what Iben & Renzini (1983) have called the early asymptotic branch (EAGB) will be discussed here alone because of the difficulty in isolating members of the thermally pulsing asymptotic branch (TPAGB, e.g., Eggen 1992). Figure 1 represents the EAGB and RHB relations in the $(b-y, c_1)$ plane, from Anthony-Twarog & Twarog (1994, AT&T). A section of the giant and subgiant branch for $[Fe/H] = -1.5$ dex is also represented. Obviously separation of normal giants and AGB stars redder than about $(b-y)_0 = 0.70$ mag is difficult. The lack of sensitivity of the $b-y$ and c_1 colors for the AGB and RHB stars, to metallicity variations, will be discussed below. For reasons which will become clear later, the RHB stars discussed here have $(b-y)_0$ between 0.25 and 0.47 mag, whereas AGB stars are limited to $(b-y)_0 = 0.47-0.70$ mag. The stars were selected from a catalogue of BD and CPD stars with Strömgren photometry, as well as accurate proper motions and radial velocities. Except for a half dozen stars, the visual magnitudes are brighter than 10.

The 61 stars represented by clear circles in Fig. 1 are listed in Table 1, which also contains the mean values of $(b-y)$, c_1 , and m_1 , obtained from all available sources (see

references in Eggen 1997a). The calcium index, hk , is from Twarog & Anthony-Twarog (1995), the DDO photometry is mainly from Norris *et al.* (1985) and my own unpublished results and the spectral types are mainly from Houk (e.g., 1982). The reddening determinations are from AT&T, who used the reddening maps of Burstein & Heiles (1982), or are based on Strömgren and $H\beta$ photometry of stars in the immediate vicinity.

The values of $P[Fe/H]$, obtained from the calibration of m_1 and $b-y$ by AT&T are listed in Table 2. The $(b-y)_0$ and $(R-I)_0$ colors of the RHB and AGB members of the two halo groups (Eggen 1997a), Kapteyn's star and Ross 451, are listed in Table 3 together with stars from Table 1 for

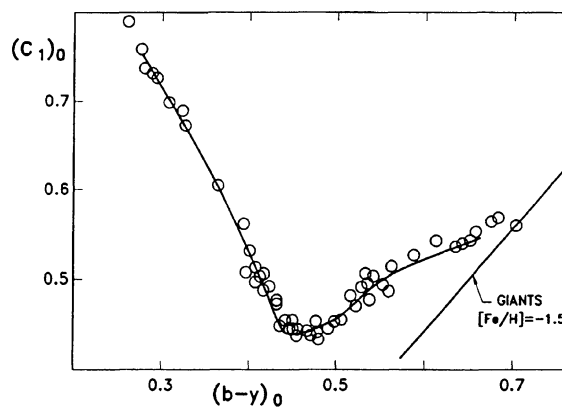


FIG. 1. The $(b-y, c_1)$ relation for RHB and AGB stars.

¹Cerro Tololo Inter-American Observatory, National Optical Astronomy Observatories, operated by the Association of Universities for Research in Astronomy, Inc. (AURA Inc.), under cooperative agreement with the National Science Foundation.

TABLE 1. RHB and AGB stars near the Sun.

HD DM	$E(b-y)$	$(b-y)_0$	$(m_1)_0$	$(C_1)_0$	$(hk)_0$	$(42-48)_0$	$(C_m)_0$	Sp.T
20	0 ^m .006	0 ^m .429	0 ^m .093	0 ^m .472	0 ^m .453			F2 V
-23.72	0.012	0.447	0.137	0.458	0.609			
2796	0.005	0.538	0.070	0.504	0.415	1 ^m .686	-0 ^m .054	FW
3179	0.007	0.444	0.147	0.444	0.628	1.659	-0.004	F8 V
-11.145	0.024	0.580	0.107	0.515	0.520			
6229	0.020	0.469	0.152	0.455				G0 V
6268	0.012	0.587	0.091	0.524	0.492	1.724	-0.090	FW
8189	0.025	0.451	0.134	0.457	0.619			G2WF5
13979	0.000	0.503	0.057	0.453	0.313	1.580	-0.034	F/GW
-22.395	0.020	0.534	0.111	0.475	0.590			
17072	0.008	0.432	0.136	0.450	0.591	1.637	0.007	G2WF5
21022	0.000	0.651	0.142	0.537	0.678	1.871	-0.101	G6 V W
24961	0.005	0.480	0.196	0.432				G8 III-IV
25532	0.053	0.424	0.109	0.496	0.472	1.558	0.032	gF5
-70.353	0.050	0.293	0.087	0.719	0.289			
34048	0.001	0.400	0.100	0.532		1.534	0.090	G0WF2
38893	0.026	0.453	0.158	0.443		1.685	0.003	G3WF8
46549	0.027	0.450	0.172	0.447				G3WF7
47147	0.030	0.280	0.08	0.731	0.190	1.310	0.132	A2/5W
49608	0.010	0.520	0.223	0.471	0.933			
82590	0.029	0.309	0.082	0.698	0.317	1.410	0.068	F6WA9
83212	0.018	0.676	0.250	0.571	0.993	2.011	-0.062	G8 III WF7
+54.1323	0.003	0.467	0.096	0.440				
88332	0.017	0.500	0.257	0.447	0.777			
-30.8626	0.034	0.487	0.119	0.472	0.584	1.686	-0.033	
-37.7677	0.050	0.526	0.143	0.519	0.646	1.751	-0.081	
105546	0.000	0.471	0.106	0.438				G2 IV
106373	0.044	0.294	0.044	0.723	0.196			A5W
107752	0.025	0.561	0.071	0.479	0.406			
110885	0.000	0.422	0.098	0.492	0.481			
+3.2782	0.015	0.655	0.155	0.558				
117327	0.200	0.271	0.107	0.750	0.254			F7WF8
+18.2757	0.000	0.550	0.070	0.490				
119516	0.000	0.407	0.056	0.512				
121135	0.008	0.524	0.121	0.512	0.656			
122563	0.000	0.640	0.095	0.531	0.488	1.799	-0.084	F8 IV
124358	0.031	0.599	0.138	0.534	0.683			
+9.2860	0.003	0.447	0.087	0.453	0.440			
+9.2870	0.012	0.629	0.110	0.534	0.681			
+11.2998	0.045	0.417	0.098	0.506				
+9.3223	0.041	0.436	0.050	0.475	0.326			
150875	0.025	0.398	0.107	0.561				
+17.3248	0.040	0.454	0.073	0.437	0.387			
159370	0.070	0.341	0.095	0.664		1.388	0.158	
166161	0.209	0.475	0.132	0.458	0.594	1.759	-0.044	
+25.3410	0.060	0.376	0.076	0.559				
184266	0.039	0.386	0.065	0.602	0.320			F2 V
186218	0.042	0.493	0.152	0.446		1.787	-0.011	G3WF6 V
195636	0.044	0.422	0.026	0.464	0.217			
-3.5215	0.032	0.403	0.089	0.493	0.429			
204543	0.024	0.609	0.156	0.551	0.733			
-9.5831	0.017	0.628	0.159	0.537	0.782			
214362	0.006	0.364	0.065	0.601	0.281	1.446	0.048	GW
215601	0.009	0.529	0.147	0.494		1.769	-0.046	G6WF3
216143	0.013	0.672	0.161	0.562	0.698			
217808	0.009	0.510	0.088	0.480	0.488			G4WA/F
220662	0.006	0.678	0.198	0.568	0.867			F8/G3
221580	0.000	0.470	0.128	0.430		1.649	-0.036	G8WF
222434	0.007	0.701	0.236	0.553	0.941			G2/3 V
222925	0.000	0.404	0.114	0.496		1.534	0.020	Ap
223740	0.000	0.542	0.214	0.481				G6WG0 IV

which $R-I$ values are available. The colors are correlated in Fig. 2. The $(R-I)$ system is defined in Eggen (1982). From line-blanketing considerations (e.g., Sandage & Eggen 1959) the range of $P[\text{Fe}/\text{H}]$ between -0.85 and -2.55 dex in Table 3 should induce a range of about 0.025 mag in $(b-y)_0$, for a given $(R-I)_0$, whereas the scatter in Fig. 2

appears considerably less than this. In fact the results for a sample of giants and subgiants discussed by AT&T is shown in Fig. 3 where the scatter in $(b-y)_0$, at a given $(R-I)_0$, is 0.02–0.05 mag. The negligible blanketing in $(b-y)$ for RHB and AGB stars may be related to the difference between the atmospheres of the dwarfs and of the EAGB stars,

TABLE 2. Photometric and astrometric parameters for stars in Table 1.

HD DM	μ_p/μ_0 0.001	ρ km/sec	V_0	MOD	U	V km/sec	W	P[Fe/H] dex	(B-V) ₀
20	134/-45	-57.4	9.03	9.03	+299	-311	-16	-1.66	0.58
-23.72	-26/-25	+20.2	9.54	8.48	+22	-77	-33	-1.12	0.61
2796	-7/-61	-60.5	8.40	8.94	-109	-151	+29	-2.20	0.745
3179	40/-33	-74.5	9.71	8.61	+42	-130	+60	-0.92	0.605
-11.145	-	-93.4	10.71	11.27	-	-	-	-2.10	0.781
6229	18/-25	-96.0	8.51	7.51	-35	-96	-87	-1.09	0.64
6268	-21/-40	+38.4	8.07	8.91	-114	-60	-72	-2.25	0.82
8189	43/-19	-	9.31	8.31	-	-	-	-1.15	0.615
13979	31/-63	+60.7	9.19	9.90	-76	-314	-26	-2.55	0.695
-22.395	-26/-36	+103.1	10.44	10.77	-246	-82	-185	-2.00	0.74
17072	-67/-14	+62.6	6.51	5.24	+2	-68	-25	-1.00	0.585
21022	34/-36	+113.0	9.20	10.07	-18	-274	-2	-1.90	0.92
24961	6/-40	-5.2	8.39	7.31	-16	-48	-25	-0.90	0.66
25532	87/14	-112.5	7.98	7.88	-71	-270	+10	-1.50	0.875
-70.353	32/126	+180.0	9.58	9.08	+367	-220	-108	-1.60	0.375
34048	50/-43	+255.0	9.99	9.79	+196	-294	-40	-1.50	0.54
38893	3/24	+122.0	9.40	8.30	+43	-111	-60	-0.86	0.62
46549	-	-	9.28	8.28	-	-	-	-0.85	0.615
47147	78/-49	+291.0	9.07	8.50	-71	-356	+26	-1.7	0.365
49608	-5/4	-	7.75	6.92	-	-	-	-0.90	0.72
82590	36/-141	+215.6	9.33	8.00	-198	-352	-57	-1.70	0.40
83212	-18/-21	+111.0	9.25	9.88	+30	-147	-72	-1.40	0.96
+54.1323	13/-32	-65.8	9.32	9.13	-66	-109	+1	-1.85	0.64
88332	-5/-12	-	7.52	6.32	-	-	-	-0.65	0.69
-30.8626	-9/-43	+264.0	9.57	9.47	-69	-301	-31	-1.67	0.67
-37.7677	-11/-9	+190.0	9.35	9.60	-50	-182	+37	-1.60	0.735
105546	-32/-63	+19.3	8.67	8.60	+26	-158	+85	-1.75	0.645
106373	-101/27	+96.0	8.73	8.50	+200	-159	+72	-2.63	0.38
107752	-	+220.0	9.89	11.09	-	-	-	-2.65	0.78
110885	-6/-50	-28.9	9.17	8.97	-51	-110	-90	-1.50	0.57
+3.2782	-24/-14	+32.3	9.64	10.55	+95	-112	+30	-1.95	0.925
117327	-	-	8.43	7.73	-	-	-	-1.70	0.355
+18.2757	-28/-31	-22Var	9.64	10.54	+28	-254	-21	-2.52	0.765
119516	-52/-21	-287.0	9.08	8.93	+161	-130	-257	-2.20	0.545
121145	-39/-20	+126.4	9.34	9.59	+17	-179	+115	-1.85	0.775
122563	-195/-74	-26.0	6.20	7.56	+164	-277	+23	-2.45	0.90
124358	-93/-33	+323.0	9.37	10.01	+56	-499	+270	-1.95	0.84
+9.2860	-	-19.0	10.82	10.72	-	-	-	-1.85	0.61
+9.2870	-67/0	-120.7	9.38	10.54	+337	-259	+26	-2.35	0.885
+11.2998	-110/-56	+50.2	8.87	8.62	-46	-226	+165	-1.50	0.565
+9.3223	-	+67.0	9.07	9.05	-	-	-	-2.40	0.59
150875	-3/7	-	8.22	7.67	-	-	-	-1.20	0.535
+17.3248	-49/-24	-145.6	9.17	9.07	+55	-212	+36	-2.15	0.62
159370	6/-1	-	9.40	8.50	-	-	-	-1.44	0.385
166161	-96/-189	+70.5	7.24	7.34	-169	-252	-3	-1.50	0.655
+25.3410	-12/-34	-	9.14	8.74	-	-	-	-1.80	0.50
184266	130/-200	-348.8	7.43	7.03	+313	-293	-135	-2.00	0.515
186218	-31/-47	-	9.45	8.85	-	-	-	-1.30	0.68
195636	-74/-111	-256.0	9.36	9.36	-48	-412	+165	-2.60	0.57
-3.5215	-	-293.7	10.05	9.75	-	-	-	-1.55	0.54
204543	9/-48	-100.2	8.21	8.81	+10	-166	-13	-1.85	0.855
-9.5831	-1/-20	+14.5	10.34	11.07	-77	-121	-61	-1.87	0.885
214362	181/-55	-92.3	9.07	8.47	+350	-250	-145	-2.00	0.485
215601	62/-144	-42.0	8.44	8.44	+42	-363	-23	-1.60	0.735
216143	-70/-107	-114.3	7.77	8.80	-263	-244	+73	-1.95	0.95
217808	30/-21	+155.0	9.29	9.71	+15	-135	-167	-2.20	0.705
220662	14/-24	-79.1	10.08	10.97	+30	-212	+29	-1.75	0.96
221580	117/-74	-	9.20	9.00	-	-	-	-1.45	0.645
222434	0/-51	+13.4	8.79	9.69	-85	-192	+10	-1.56	0.995
222925	158/-104	-38.0	9.01	7.96	+229	-261	+59	-1.06	0.545
223740	27/-57	-	9.06	8.45	-	-	-	-0.99	0.755

which are defined by models with an electron-degenerate carbon-oxygen core, a helium-burning shell, and extinct hydrogen-burning shell. Nevertheless, the values of $P[\text{Fe}/\text{H}]$ obtained from m_1 (Table 2) are confirmed by well-determined spectroscopic values listed in Table 4. Possibly,

the validity of m_1 vs $(b-y)$ is maintained because $m_1 = (v - b) - (b - y)$. The mean relation in Fig. 2, based on the members of the two halo groups ($[\text{Fe}/\text{H}] = -1.65$ dex) is

$$(b-y)_0 = 1.48 (R-I)_0 + 0.045. \quad (1a)$$

TABLE 3. Correlation of $(R-I)_0$ and $(b-y)_0$ for AGB and RHB stars.

HD DM	E(b-y)	(b-y) ₀	(R-I) ₀	[Fe/H] dex	HD DM	E(b-y)	(b-y) ₀	(R-I) ₀	[Fe/H] dex
Kapteyn's Star Group					Ross 451 Group				
21022	0 ^m .000	0 ^m .651	0 ^m .404	(-1 ^m .65)	34048	0 ^m .001	0 ^m .400	0 ^m .260	(-1 ^m .65)
25572	0.053	0.424	0.255		82590	0.029	0.309	0.180	
215601	0.009	0.528	0.328						
-30.8626	0.034	0.000	0.310						
2796	0.005	0.538	0.351	-2.20	-37.7677	0.95	0.526	0.316	-1.50
6229	0.020	0.469	0.296	-1.09	124358	0.031	0.507	0.316	-1.95
6268	0.012	0.587	0.362	-2.25	159730	0.040	0.341	0.201	-1.44
13979	0.000	0.503	0.321	-2.55	166161	0.209	0.475	0.290	-1.50
17072	0.008	0.432	0.276	-1.00	184266	0.039	0.386	0.244	-2.00
					186218	0.042	0.493	0.299	-1.30
-20.353	0.050	0.293	0.184	-1.60	214362	0.006	0.364	0.232	-2.00
34048	0.001	0.400	0.259	-1.50	215601	0.009	0.528	0.335	-1.60
38893	0.026	0.453	0.280	-0.86	217808	0.009	0.510	0.330	-2.20
46549	0.037	0.450	0.282	-0.85	222925	0.000	0.404	0.245	-1.06
83212	0.018	0.676	0.425	-1.40	223740	0.000	0.542	0.320	-0.99
122563	0.000	0.640	0.414	-2.45					

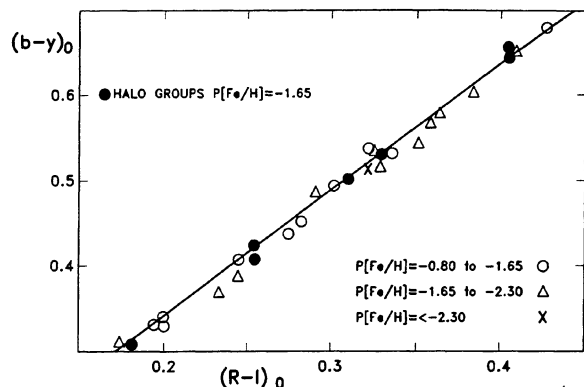


FIG. 2. $(b-y)$, $(R-I)$ relation for RHB and EAGB stars.

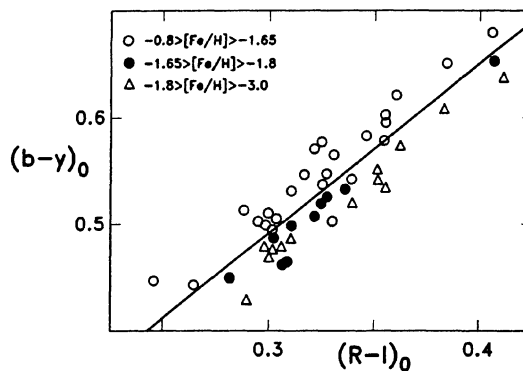


FIG. 3. Same as Fig. 2 for halo giant and subgiant stars.

TABLE 4. Comparison of well-determined spectroscopic abundances of heavy elements with the values obtained from Strömgren Photometry.

HD DM	P[Fe/H] dex	[Fe/H] dex	HD DM	P[Fe/H] dex	[Fe/H] dex		
2796	-2.20	-2.51 (1)	107752	-2.65	-2.60 (5)		
6268	-2.25	-2.58 (1)	+9.2870	2.35	-2.39 (8)		
13979	-2.55	-2.65 (1)	195636	-2.90	-2.79 (6)		
25532	-1.50	-1.23 (8)	-35215	-1.55	-1.57 (2)		
63212	-1.40	-1.51 (2)	204543	-1.85	-1.63 (7)	-1.77 (6)	1.83 (3)
+54.1323	-1.85	-1.65 (8)	216143	-1.95	-2.10 (6)	-2.24 (3)	
105546	-1.75	-1.60 (4)	220662	-1.75	-1.59 (8)		

Notes to TABLE 4.

- (1) McWilliam, et al. 1995
- (2) Gilroy, et al. 1988
- (3) Gratton 1989
- (4) Sneden 1974
- (5) Luck and Bond 1985
- (6) Gratton and Sneden 1988
- (7) Luck and Bond 1981
- (8) AT&T

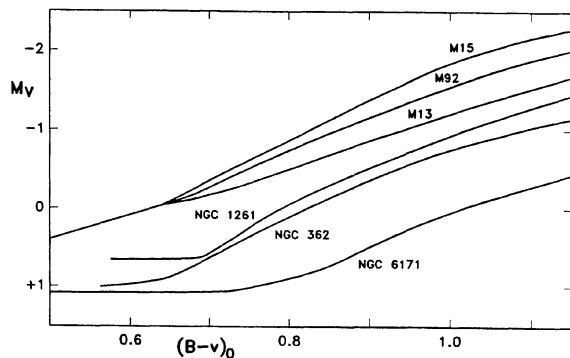


FIG. 4. Fiducial red horizontal and early asymptotic giant branches for selected globular clusters.

With $E(R-I)/E(b-y)=0.93$, this can be written as

$$E(b-y) = 3.84 (R-I) - 2.66 (b-y) + 0.120. \quad (1b)$$

Most of the stars in Table 3 have such small reddening values that a meaningful comparison with the results from Eq. (1b) is lost in the photometric errors. However, the largest value of $E(b-y)=0.209$ mag for HD 166161 is matched by 0.208 mag from Eq. (1b).

The observed red horizontal and asymptotic giant branches of representative globular clusters are shown in Fig. 4. The origins of the observations and the photometric parameters are listed in the notes to Table 5. The branches have been transferred to the $(M_V, [Fe/H])$ plane. For the clusters with $[Fe/H] < -1.00$ dex, the stars redder than about $(B-V)_0 = 0.65$ mag represent the AGB and for them,

$$M_V = 5.05 - 4.70 (B-V)_0 + (1.34 - 0.5(B-V)_0)[Fe/H]. \quad (2)$$

This relation reconstructs the individual cluster values remarkably well, indicating that the relative spacing of the clusters (i.e., the differential distances) are approximately correct. For example, treating the published mean points for the observed red horizontal and asymptotic giant branches as individual stars, together with the reddening values listed in

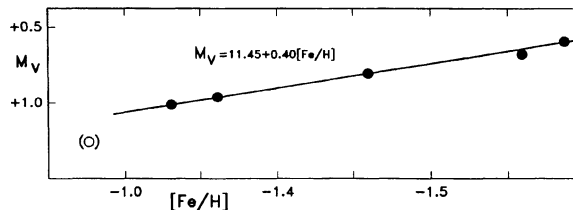


FIG. 5. $M_V, [Fe/H]$ relations for the cluster variables.

Table 5, leads to mean moduli of 13.9 ± 0.07 (M13), 14.27 ± 0.06 (M92), and $15.85 \pm 0.002(\sigma)$ mag (NGC 1261). The luminosities for the AGB stars in Table 2 are from Eq. (2) and for the RHB stars from Fig. 4.

The relationship between $[Fe/H]$ of the cluster stars and the mean luminosity of the cluster variables is shown in Fig. 5. Not unexpectedly, because the photometric parameters are basically those published by Sandage (1993), the value of $dM_V(RR)/d[Fe/H]$ is very similar to that found by Sandage (1990): 0.040 compared with 0.39. Sandage (1993) later derived a slope of 0.30, which is considerably larger than that determined from Baade-Wesselink analyses (see Walker 1995 for references). The view has here been adopted that $[Fe/H] \sim -0.9$ dex marks the halo-disk boundary and this is not disproved by Fig. 4, where an obvious change occurs in the structure of the HB+AGB between NGC 362 ($[Fe/H] = -1.13$ dex) and NGC 6171 (-0.8 dex). NGC 6171 is near the top of a hierarchy of similar branches, including those of M71 (-0.7 dex), 47 Tuc (-0.65 dex), M67 (-0.15 dex), and the HR 1614 supercluster and group ($+0.10$ dex). At the abundance level of NGC 6171 the RHB has an extent of about 0.25 mag in $B-V$, centered near $B-V=0.6$ mag (Sandage & Rogues 1984), and this has shortened to about 0.13 mag in 47 Tuc, centered near $B-V=0.8$ mag (Hesser *et al.* 1987) and to no more than 0.1 mag in $B-V$ centered near $B-V=1.05$ for M67 (Eggen & Iben 1989). In the overabundant, HR 1614 supercluster and group the HB has become merely a ‘‘clump’’ with a spread of 0.02 or 0.03 mag in $B-V$ centered near $B-V=1.08$ mag (Eggen 1996). The extent of the RHB will of course be partially dependent on

TABLE 5. Origins of globular cluster observations and photometric parameters.

Cluster M	NGC	E(B-V)	(m-M) ₀	[Fe/H] dex	M _V (RR)		Reference
					OBS	COMP	
15	7078	0.08	14.95	-2.15	+0.59	+0.59	1, 2
92	6341	0.02	14.30	-2.05	+0.69	+0.63	1, 2
13	6205	0.03	13.97	-1.65	+0.75	+0.79	1, 2
	1261	0.00	16.05	-1.25	+0.95	+0.95	3, 5
	362	0.06	14.26	-1.13	+0.98	+1.00	2, 4
	6171	0.31	14.71	-0.80	+1.2:	-	6

References

1. Sandage (1970)
2. Sandage (1982)
3. Ferraro, *et al.* (1993)
4. Bolte (1989)
5. Bolte and Marleau (1989)
6. Sandage and Roques (1984)

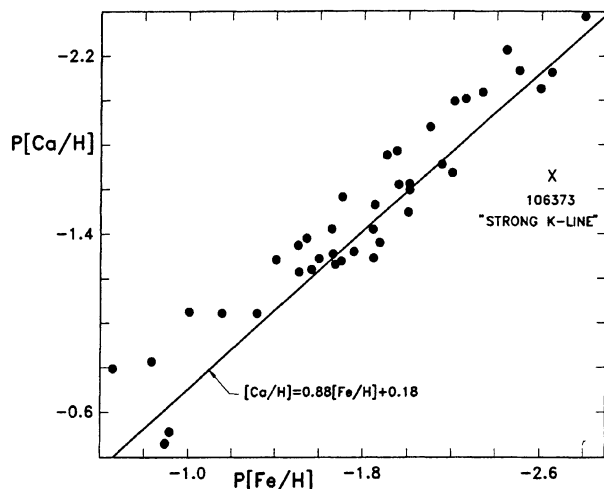


FIG. 6. Comparison of $P[\text{Ca}/\text{H}]$ and $P[\text{Fe}/\text{H}]$ for stars in Table 6.

the star density of the cluster. The short RHB in M67 and the clump in HR 1614 group are both near $M_v = +0.75$ mag. The distance modulus of NGC 6171 adopted in Table 5 (Fig. 4) is that in the current literature but, as will be discussed elsewhere in connection with the RHB stars of the old disk population, this is probably about 0.5 mag too faint. Individual luminosities for USPC (RR Lyr) variables (Eggen 1994) support the larger slope for the $dM_v(\text{RR})/d[\text{Fe}/\text{H}]$ relation. Although the validity of Eq. (2) indicates that the relative distances of the clusters are nearly correct, Reid's (1997) recent suggestion for a 0.50–0.55 mag increase in three of the clusters used here makes an adjustment to the zero point of Eq. (2) dependent upon confirmation of these increases.

The lack of blanketing in $(b-y)$ and the fact that $d(hk)/d[\text{Fe}/\text{H}] = 0.362$, for the RHB and EAGB stars, leads to

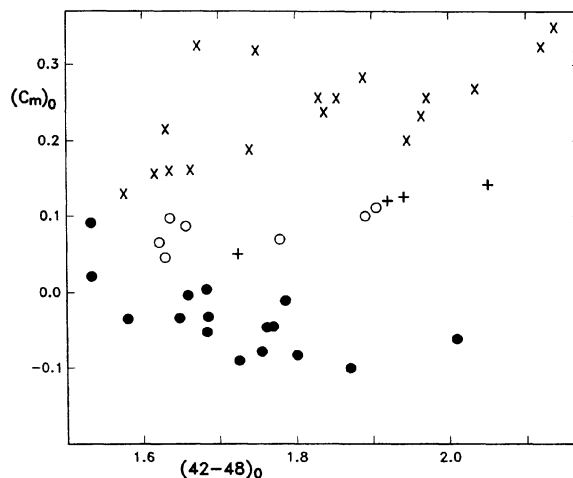


FIG. 7. Dependence of the gravity corrected CN strengths, C_m , on $(42-48)$ for RHB and AGB stars of the halo (filled circles) and old disk (open circles) populations, for well observed stars in 47 Tuc (plus signs) and members of the HR 1614 group (crosses).

$$P[\text{Ca}/\text{H}] = [(hk)_0 \text{ OBS} - (hk)_0 \text{ COMP}] / 0.362 + 0.10 \text{ dex}, \quad (3)$$

where

$$(hk)_0 \text{ COMP} = 1.55(b-y)_0 + 0.335 \text{ mag}$$

(Eggen 1997b). The resulting abundances are listed in Table 6, together with those obtained for $[\text{Fe}/\text{H}]$ using Strömgren photometry (Table 2). The abundances are compared in Fig. 6, where the straight line represents $[\text{Ca}/\text{H}] = 0.88[\text{Fe}/\text{H}] + 0.118$, derived in Eggen (1997b) from high velocity subgiant and giant stars. There may be more scatter in Fig. 6 than in the corresponding comparison for giants and subgiants, and our lack of a detailed knowledge of the line-blanketing may be a partial cause.

TABLE 6. Values of $P[\text{Ca}/\text{H}]$ from Eq. (3) and $P[\text{Fe}/\text{H}]$ from Strömgren Photometry for RHB and EAGB stars in Tables 1 and 2.

HD DM	$P[\text{Ca}/\text{H}]$ dex	$P[\text{Fe}/\text{H}]$ dex	HD DM	$P[\text{Ca}/\text{H}]$ dex	$P[\text{Fe}/\text{H}]$ dex	HD DM	$P[\text{Ca}/\text{H}]$ dex	$P[\text{Fe}/\text{H}]$ dex
20	-1.41	-1.66	49608	-0.47	-0.90	+17.3248	-1.70	-2.15
-23.72	-1.06	-1.31	8590	-1.27	-1.70	166161	-1.22	-1.50
2796	-1.98	-2.20	88332	(-0.80)	-0.65	184266	-1.59	-2.00
3179	-0.52	-0.92	-30.8626	-1.30	-1.67	195636	-2.03	-2.60
-11.145	-1.87	-2.10	-37.7677	-1.29	-1.60	-3.5215	-1.37	-1.55
6268	-1.98	-2.25	106373 ^a	(-1.64)	-2.63	204543	-1.41	-1.85
8189	-1.04	-1.15	107752	-2.10	-2.64	-9.5831	-1.35	-1.87
13979	-2.11	-2.55	110885	-1.30	-1.50	214362	-1.60	-2.00
-22.395	-1.45	-2.00	117327	(-1.28)	-1.20	216143	-1.77	-1.95
17072	-1.05	-1.00	121135	-1.26	-1.85	217208	-1.66	-2.20
21022	-1.74	-1.90	122563	-2.21	-2.45	220662	-1.33	-1.75
25532	-1.34	-1.50	124358	-1.60	-1.95	222434	-1.23	-1.56
-70.353	-1.28	-1.60	+9.2860	-1.52	-1.85			
47147	-1.60	-1.7:	+9.2870	-2.04	-2.35			

^a 106373 Strong K-line at 4226, Houk (1982).

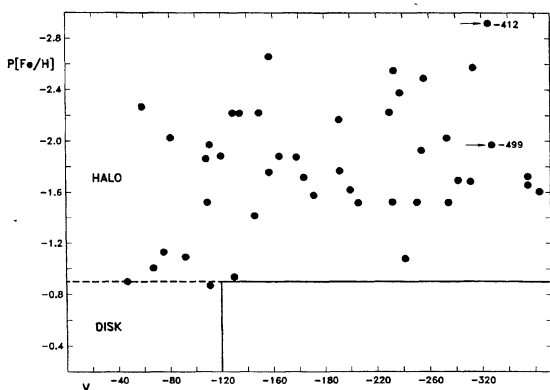


FIG. 8. Distribution of RHB and EAGB stars in the $[Fe/H]$, V -velocity plane.

The separation between disk and halo stars, which may be seen in the structure of the RHB, adds support to a previous suggestion of this separation as seen in the difference, for both giants and dwarfs, of the dependence of mean CN abundance on temperature (e.g., Eggen 1997a). Stars with $[Fe/H] > -0.9$ dex show an increase in CN strength with decreasing temperature, whereas for $[Fe/H] < -0.9$ dex the reverse is true. The stars in Tables 1 and 2 with available data are shown in the $(C_m)_0$, $(42-28)_0$ plane of Fig. 7 where open circles represent the objects with $[Fe/H] > -0.9$ dex and

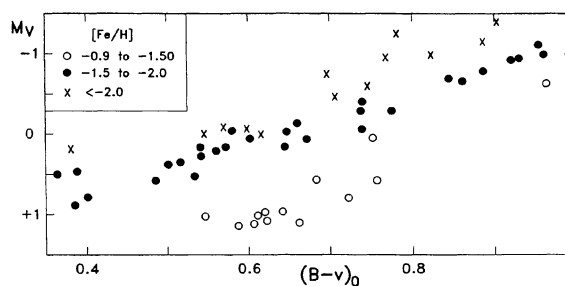


FIG. 9. Color-luminosity array from stars in Table 2.

filled circles those with $[Fe/H] < -0.9$ dex. Members of the HR 1614 group (Eggen 1996) are represented by crosses and a few well-observed giants in the old disk, 47 Tuc cluster (e.g., Eggen 1997a) are represented by plus signs. The values of C_m represent a gravity free index of the CN abundance.

The distribution of the V velocities (with respect to the sun and positive in the direction of galactic rotation) with $P[Fe/H]$ is shown in Fig. 8. The domains of disk and halo objects (Eggen 1997a, 1997b) are labeled in the figure. Meridian circle based proper motions (e.g., Carlsberg 1994) are available for the majority of the stars. Proper motions for six, and radial velocities for 12, stars are not available. Figure 9 contains the color-luminosity array, coded for values of $P[Fe/H]$.

REFERENCES

- Anthony-Twarog, B., & Twarog, B. 1994, *AJ*, 107, 1577 (AT&T)
 Bolte, M. 1989, *AJ*, 97, 1688
 Bolte, M., & Marleau, F. 1989, *PASP*, 101, 1098
 Burstein, D., & Heiles, C. 1982, *AJ*, 87, 1165
 Carlsberg 1994, *Carsberg Meridian Catalogue*, No. 8, Copenhagen Univ. Obs.
 Eggen, O. J. 1982, *ApJS*, 50, 221
 Eggen, O. J. 1992, *AJ*, 104, 275
 Eggen, O. J. 1994, *AJ*, 107, 2131
 Eggen, O. J. 1996, *AJ*, 112, 1595
 Eggen, O. J. 1997a, *AJ* (in press)
 Eggen, O. J. 1997b, *AJ* (in press)
 Eggen, O. J. & Iben, Jr., I. 1989, *AJ*, 97, 431
 Ferraro, F., Clementini, G., Fusi Pecci, F., Vitarello, E., & Buonanno, R. 1993, *MNRAS*, 264, 273
 Gilroy, K. K., Sneden, C., Pilachowski, C., & Cowan, J. 1988, *ApJ*, 327, 298
 Gratton, R. 1989, *A&A*, 215, 86
 Gratton, R., & Sneden, C. 1988, *A&A*, 204, 193
 Hesser, J., Harris, W., Vandenberg, D., Allwright, J., Shott, P., & Stetson, P. 1987, *PASP*, 99, 739
 Houk, N. 1982, *Michigan Catalogue of Spectral Types*, Vol. 4, University of Michigan
 Iben, Jr., I., & Renzini, A. 1983, *ARA&A*, 21, 271
 Luck, R., & Bond, H. 1981, *ApJ*, 249, 919
 Luck, R., & Bond, H. 1985, *ApJ*, 297, 559
 McWilliam, A., Preston, G., Sneden, C., & Searle, L. 1995, *AJ*, 109, 2757
 Norris, J., Bessel, M., & Pickles, M. 1985, *ApJS*, 58, 463
 Reid, N. 1997, *ApJ* (preprint)
 Sandage, A. R. 1970, *ApJ*, 162, 841
 Sandage, A. R. 1982, *ApJ*, 252, 253
 Sandage, A. R. 1990, *ApJ*, 350, 631
 Sandage, A. R. 1993, *AJ*, 106, 703
 Sandage, A. R., & Eggen, O. J. 1959, *MNRAS*, 119, 278
 Sandage, A. R., & Roques, P. 1984, *AJ*, 89, 1166
 Sneden, C. 1974, *ApJ*, 189, 493
 Twarog, B., & Anthony-Twarog, B. 1995, *AJ*, 109, 2828
 Walker, A. 1995, *PASP*, 83, 198